# MACHINABILITY OF LEAD-FREE BRASS – A COMPARATIVE STUDY

**Fredrik Schultheiss[1], Erik Lundström[1], Daniel Johansson[1], Volodymyr Bushlya[1], Jinming Zhou[1], Kent Nilsson[2], Jan-Eric Ståhl[1]**

*[1]Lund University, Division of Production and Materials Engineering, Lund, Sweden*
*[2]AB Markaryds Metallarmatur, Markaryd, Sweden*

fredrik.schultheiss@iprod.lth.se

Abstract: Convetional brass is still allowed to contain up to 3.5 wt.% lead even though lead is a hazardous metal. However, due to environmental concerns lead-free brasses are becoming increasingly available. The aim of this paper is to evaluate the machinability of a lead-free brass alloy, CuZn21Si3P, as compared to a convetionally used, lead-alloyed alternative, CuZn39Pb3. The attained results show that CuZn21Si3P has a considerably higher strength than the lead-alloyed material resulting in significantly higher cutting forces. This increase in cutting forces was found to result in more rapid deterioration of the cutting tool, raising concerns for higher manufacturing cost if not properly adressed.

Keywords: Machining, Cutting resistance, Cutting forces, Material properties.

## 1. INTRODUCTION

Lead (Pb) is a heavy metal which is toxic even at low exposure levels and has been found to have acute and chronic effects on human health. Lead is a multi-system toxicant which can have neurological, cardiovascular, renal, gastrointestinal, hematological and reproductive effects on humans. In addition, in nature lead is toxic to plants, animals and micro-organisms (UNEP, 2010). During 2003 the International Lead and Zinc Study Group (ILZSG) estimated that 115 000 tonnes of lead were used in different alloys by companies operating in the countries reporting to the ILZSG organization. This was estimated as being equivalent to 80% of the world consumption during the same time period (UNEP, 2010).

So called free-machining brass is conventionally attained through the addition of 2 to 3 wt.% lead. Even though lead is soluble in molten brass it is then participated during solidification usually forming particles 1 to 10 µm in diameter (Trent and Wright, 2000). According to Trent and Wright (2000) the addition of lead in brass greatly reduces the cutting forces as well as resulting in shorter chips and a decrease of the attained tool wear as compared to the lead-free alternative. However, due to environmental concerns the addition of lead as an alloying element in for instance brass is questionable even if considering the benefits on the attained machinability. Efforts to decrease the Pb contents in brass have previously been performed by several different researchers. Attempts through using for example bismuth have been reported (La Fontaine, *et al.*, 2006), however, the high price of bismuth has discouraged any wider use of this alloying element. Another possible alloying element which has been investigated is silicon although this is believed as resulting in a decrease of the machinability as compared to the lead alloyed alternative (Taha, *et al.*, 2012). Some authors have also proposed the addition of titanium in bismuth alloyed brasses (Li, *et al.*, 2011). Even though this addition was proven to have a favorable influence on the machinability it is unclear how attractive this solution would be for general implementations since this could be expected to increase the price of the attained brass material.

In this paper the machinability of two commercially available brasses are compared. One of the investigated brasses is the lead alloyed CuZn39Pb3 which is traditionally used in industry for several different applications. The lead-free alternative used in this investigation was CuZn21Si3P which contains only trace amounts of lead.

In CuZn21Si3P the lead has been substituted by the addition of 3 wt.% silicon. Thus far little is however known on the influence on the machinability attained through this substitution.

## 2. MATERIAL PROPERTIES

Brass is a widely used alloy characterized by its good corrosion resistance, good wear properties as well as high thermal and electrical conductivity. As a result brasses are widely used for a range of different applications such as electrical and automotive components as well as valves and fittings (Garcia, *et al.*, 2010).

Brass is a copper alloy containing zinc and potentially other alloying elements. Generally brass will consist of 55 wt.% Cu or more, a ratio which could be varied depending on the desired material characteristics. Lead is commonly added in brass alloys intended for machining purposes as a method of increasing the materials machinability (Brennert, 1993). The nominal chemical composition for each of the two investigated materials can be found in Table 1. Examples of the microstructure for each of the investigated materials can be found in Fig. 1.

Table 1. Chemical composition according to nominal standards (wt.%), (Wieland-SW1, 2014; Wieland-Z32/Z33, 2014).

| Material | Cu | Zn | Pb | Si | P |
|---|---|---|---|---|---|
| CuZn39Pb3 | 57.3 | Balance | 3.3 | - | - |
| CuZn21Si3P | 76 | Balance | - | 3 | 0.05 |

Fig. 1. Examples of the microstructure of the two investigated materials; CuZn39Pb3 (left) and CuZn21Si3P (right).

Through comparing the microstructure of each of the two materials by using the SEM images found in Fig. 2 it is possible to observe that collections of lead may be found throughout the material for the lead-alloyed CuZn39Pb3 material. It is also of interest to note that even the minute traces of lead can be observe in some areas of the otherwise lead-free CuZn21Si3P material.

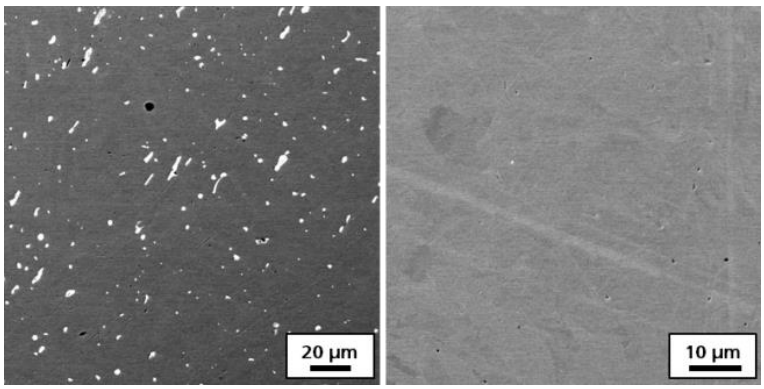


Fig. 2. Examples of the distribution of lead in the microstructure of CuZn39Pb3 (left) and CuZn21Si3P (right).

*2.1. Tensile strength*

As part of this investigation tensile tests were performed on the investigated brass materials, Fig. 3. The tensile tests were performed in one direction in accordance to SS-EN 10 002-1.

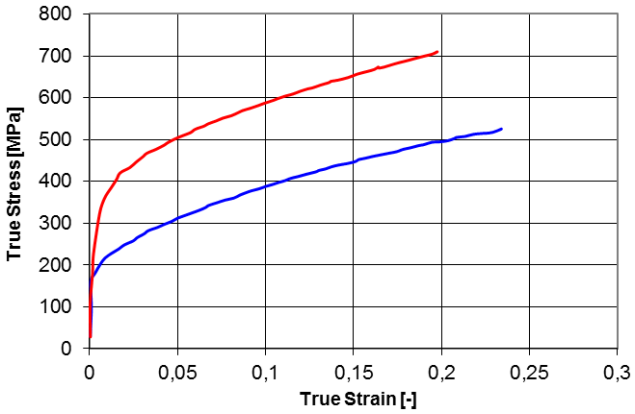


Fig. 3. Attained tensile strength; CuZn39Pb3 (blue) and CuZn21Si3P (red).

As can be seen from the obtained results a considerable difference may be noted between the two investigated materials in this comparison. A summary of the attained material properties from this evaluation can also be found in Table 2.

Table 2. Material properties attained during the current tensile tests.

| Material property | CuZn39Pb3 | CuZn21Si3P |
|---|---|---|
| Yield strength [MPa] | 201 | 342 |
| Tensile strength [MPa] | 525 | 717 |
| Elongation at rupture [%] | 26 | 22 |

*2.2. Hardness and abrasiveness*

In order to evaluate the hardness of the two different brass materials micro-hardness indentations were performed at randomly selected positions of the bulk material while using a load of 100 mN and a Berkovich indenter. In total 64 individual indentations were performed in each material, the mean value of which can be found in Table 3 for each material.

Table 3. Mean value of the measured micro hardness for each material.

| Material | Hardness, $H$ [GPa] |
|---|---|
| CuZn39Pb3 | 1.86 |
| CuZn21Si3P | 2.97 |

As can be seen from the obtained results presented in Table 3, CuZn21Si3P displays a considerably higher hardness as compared to the lead-alloyed CuZn39Pb3 material. As a result it could be expected that the cutting forces acquired during any machining operation will be significantly higher for the lead-free brass material, CuZn21Si3P.

In order to also evaluate the hardness variation 400 individual micro hardness indentations were performed arranged in a matrix 20 by 20 indentations in size while using a Berkovich indenter at a load of 50 mN. The attained results are presented in Fig. 4. For both materials it was attempted to model the distribution of the attained micro hardness by using a combined distribution comprised of two Weibull distributions illustrated by the red and blue curves in the figure as compared to the measured values. Also, the two parts of the distribution is for each case illustrated by the darker, numbered curves. In both cases an accuracy better than 1% were attained between the model and measured values. As can be seen in Fig. 4, based on the attained hardness results it is clear that both materials consist of two phases of differing hardness. Overall, there exists a significant difference in the micro hardness for the two different materials where the average value of the micro hardness of the lead-free material CuZn21Si3P is roughly 1 GPa larger than the equivalent value of the lead-alloyed material CuZn39Pb3. Also, note the slight peek in frequency at a low hardness (roughly $H$ = 1.4 GPa) for the lead-

alloyed material. This irregularity is believed to be due to the influence of lead in the material resulting in certain areas within the workpiece material with a significantly lower hardness.

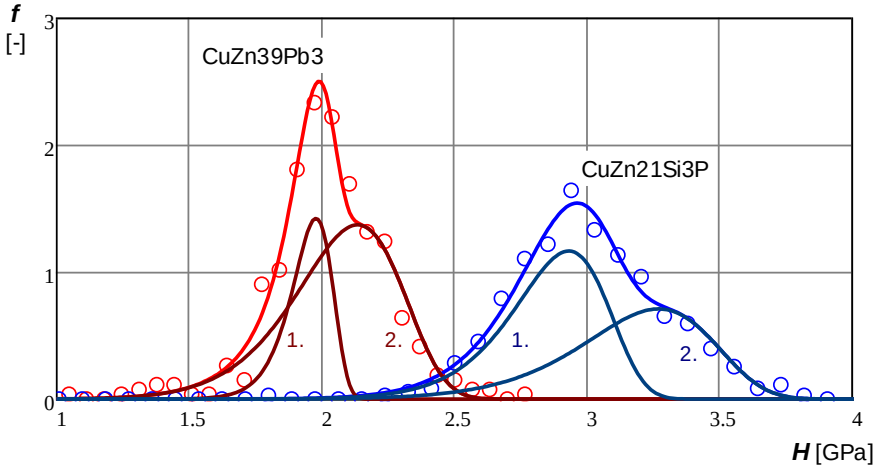


Fig. 4. Variation of the attained micro hardness *H* for the two investigated materials; CuZn39Pb3 (red) and CuZn21Si3P (blue). The darker curves 1. and 2. indicates the distribution of each of the two phases.

Through analyzing the obtained variation of the micro hardness a quantitative value of the abrasiveness was obtained as presented later in the following section, Section 2.3.

### *2.3. Polar diagram*

Previous research conducted by the authors has resulted in the introduction of so called polar diagrams for the evaluation of the potential machinability of workpiece materials (Andersson and Ståhl, 2007; Xu, *et al.*, 2013). These diagrams are intended to allow for a numerical and graphical comparison of the potential machinability of different workpiece materials as compared to a reference material. This comparison is performed through evaluating 5 different material properties which have previously been found to have a significant influence on the machining process (Andersson and Ståhl, 2007; Xu, *et al.*, 2013; Avdovic, *et al.*, 2011; Olovsjö, *et al.*, 2011; Olovsjö, *et al.*, 2012; Xu, *et al.*, 2010). The 5 material properties used as part as the polar diagram for evaluating the potential machinability of a workpiece material are:

*Ductility:* A high ductility of the workpiece material commonly results in strong adhesion between the workpiece material and cutting tool which is commonly unfavorable for the attained machinability. Also, a low ductility is generally favorable in relation to the chip formation as materials with a low ductility tend to form shorter and thus more manageable chips.

*Hardness:* The hardness of a workpiece material has a significant influence on the cutting resistance of the workpiece material during any cutting process. Thus, a high hardness will generally result in high cutting forces and as a result low hardness values are generally considered as favorable except in the case of very ductile materials.

*Thermal conductivity:* Heat is generated by the plastic deformation of the workpiece material and the friction occurring between the tool and workpiece/chip material during a metal cutting operation. In order to not risk excessive tool wear or other temperature related defects a high rate of heat removal is commonly desired. A high thermal conductivity of the workpiece material is thus beneficial through favoring the rapid conduction of heat away from the cutting zone.

*Strain hardening:* A high strain hardening value generally implies more energy being needed for chip formation, in turn resulting in the need for higher cutting forces. Thus, a high strain hardening value may commonly be seen as having a detrimental effect on the attained machinability of a workpiece material. The desire to simplify the use of the current model through only using material property data commonly available on a material certificate resulted in the introduction of a strain hardening factor $D_n$, Equation 1, which was set as equivalent to the ratio between the ultimate tensile strength $R_m$ and the yield strength $R_p$.

$$D_n = \frac{R_m}{R_p} \qquad (1)$$

*Abrasiveness:* Abrasive wear mechanisms during metal cutting will commonly have a negative effect on the tool life. Abrasive wear of cutting tools can be considered as being due to the action of hard particles of microscopic size enclosed in the workpiece material. A high content of such particles, e.g. carbides and oxides, makes the machining of these materials difficult through inhibiting bulk deformation of chip segments as well as resulting in chipping and flank wear of the cutting tool (Ren, *et al.*, 2001). Based on the previously published model for quantifying the abrasiveness of a specific material as presented by Ståhl (2012) the following model is proposed for quantifying the abrasiveness during this comparison, Equation 2. In this equation $H_{macro}$ is the macro hardness of the material and $\Delta H_{micro}$ is the difference between the largest and smallest micro hardness of the measured material within a 97.5% confidence interval. Through preforming 400 micro hardness measurements in the bulk material arranged in a matrix 20 by 20 indentations in size it was believed that sufficient knowledge of the spread in micro hardness of the workpiece material was obtained. In this comparison the macro hardness $H_{macro}$ was presumed as being the average value of all 400 micro hardness values attained for the material in question.

$$W_{ab} = H_{macro} + \Delta H_{micro} \qquad (2)$$

The following values of the material properties were used during this evaluation of the potential machinability, Table 4. In this case the thermal conductivities as stated by the material supplier were used (Wieland-SW1, 2014; Wieland-Z32/Z33, 2014).

Table 4. Material properties used for evaluating the potential machinability.

| Material property | CuZn39Pb3 | CuZn21Si3P |
|---|---|---|
| Yield strength, $R_p$ [MPa] | 201 | 342 |
| Tensile strength, $R_m$ [MPa] | 525 | 717 |
| Elongation at rupture, $\varepsilon_b$ [-] | 0.26 | 0.22 |
| Hardness, $H$ [GPa] | 1.86 | 2.97 |
| Thermal conductivity, $k_W$ [W/m·K] | 113 | 35 |
| Abrasiveness $W_{ab}$ [GPa] | 3.25 | 4.35 |
| Strain hardening factor, $D_n = R_m/R_p$ | 2.61 | 2.10 |

Through using the conventionally used, lead-alloyed CuZn39Pb3 brass as a reference the following polar diagram could be attained, Fig. 5.

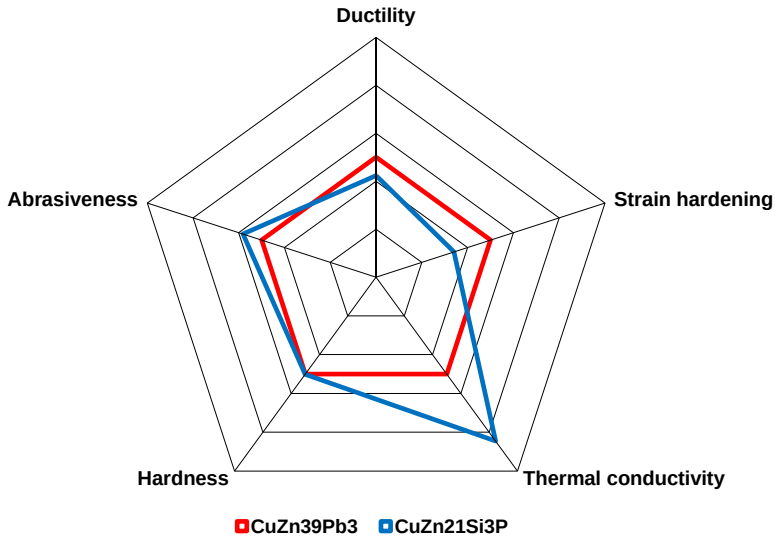


Fig. 5. Attained polar diagram while using CuZn39Pb3 as a reference material.

As can be seen in Fig. 5 almost all material properties influencing the potential machinability indicate that the lead-free material CuZn21Si3P has a worse machinability than the lead-alloyed alternative, CuZn39Pb3.

## 3. EXPERIMENTAL EVALUATION

The attained cutting forces and tool wear during longitudinal turning were measured as part of this investigation as a method for comparing the machinability of the different brass workpiece materials.

*3.1. Experimental setup*

In order to evaluate the variation in machinability between the two different materials longitudinal turning experiments were performed at a range of different cutting data. Both materials were supplied as bars having an initial diameter of approximately 50 mm. The inserts used were uncoated H10F cemented carbide DNGA150708F inserts with an edge radius of approximately 10±5 µm. An example of the tool microstructure typical for the tools used can be found in Fig. 6. The cutting speed, $v_c$, remained constant during all experiments at $v_c$ = 400 m/min while both the feed, $f$, and depth of cut, $a_p$, was varied in the range of 0.05 to 0.30 mm/rev and 0.5 to 2.5 mm respectively while measuring the cutting forces. While evaluating the tool wear as described in section 3.4 the cutting data remained constant at $v_c$ = 400 m/min, $f$ = 0.20 mm/rev and $a_p$ = 0.8 mm while only the workpiece material was varied as to attain a appropriate comparison.

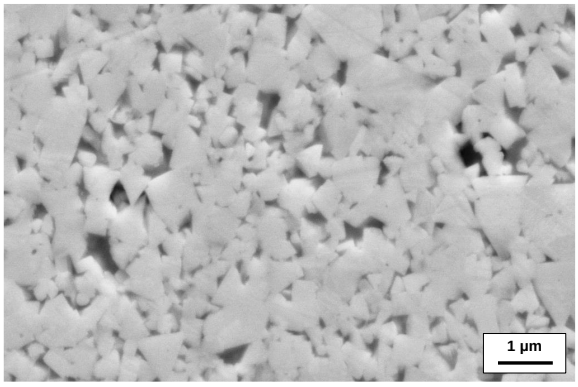


Fig. 6. Example of the tool microstructure.

*3.2. Evaluation of the obtained chips*

The obtained chips were collected and evaluated for all cutting data combinations used as previously described. A clear difference was observed while evaluating the chips from each of the two investigated materials. Fig. 7 illustrate a comparison between chips obtained from each of the two investigated workpiece materials at $f$ = 0.20 mm/rev and $a_p$ = 2.0 mm. As may be noted in Fig. 7 there is a significant difference between the chips obtained from each of the two workpiece materials. However, if considering each of the two materials separately, essentially similar chips were obtained for the whole range of cutting data investigated.

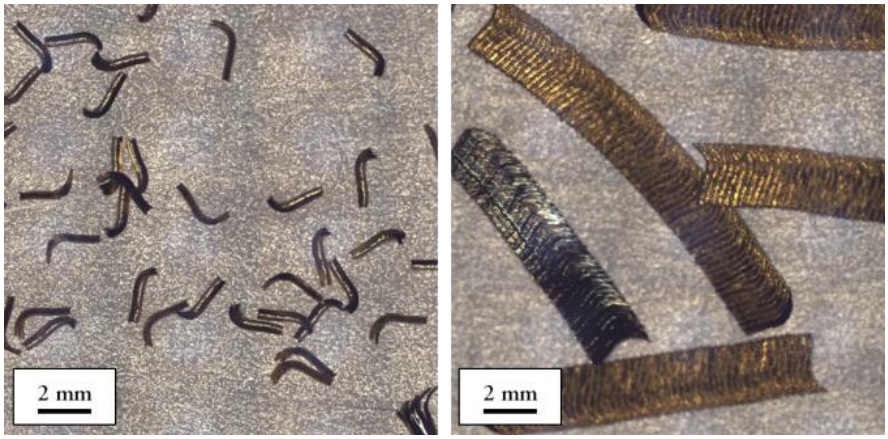


Fig. 7. Comparison of obtained chips while machining CuZn39Pb3 (left) and CuZn21Si3P (right) at $f$ = 0.20 mm/rev and $a_p$ = 2.0 mm.

As can be seen in Fig. 7 the chips obtained while machining CuZn39Pb3 were generally discontinues and thus resulting in very short chips which could easily be removed during any machining process. In contrast the machining of CuZn21Si3P resulted in long lamellar chips which although easily broken could potentially be more problematic to remove from the machining process during certain operations.

*3.3. Cutting forces and cutting resistance*

The attained cutting forces were measured during the whole test sequence in order to investigate the difference of the attained cutting forces for the two investigated materials. An example of the attained cutting forces at a depth of cut of $a_p$ = 2 mm can be found in Fig. 8. Note how all three force components; the main cutting force $F_c$, the feed force $F_f$ and the passive force $F_p$, are significantly larger for the lead-free CuZn21Si3P material for all values of the theoretical chip thickness $h_1$.

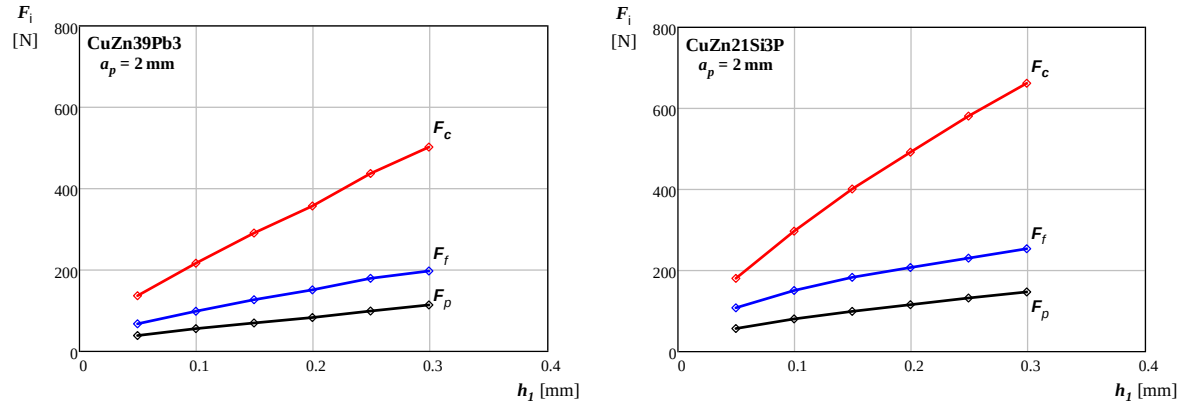


Fig. 9. Cutting forces as a function of $h_1$ for varying workpiece materials at $a_p$ = 2 mm.

Through using the attained main cutting force $F_c$ the cutting resistance $Cr$ may be calculated, Equation 3, which enables a better comparison between the different test conditions.

$$Cr = \frac{F_c}{h_1 \cdot b_1} \qquad (3)$$

In Equation 3 $h_1$ is the theoretical chip thickness and $b_1$ is the theoretical chip width. Through using this equation the cutting resistance may be calculated for each of the machining cases investigated, Fig. 10.

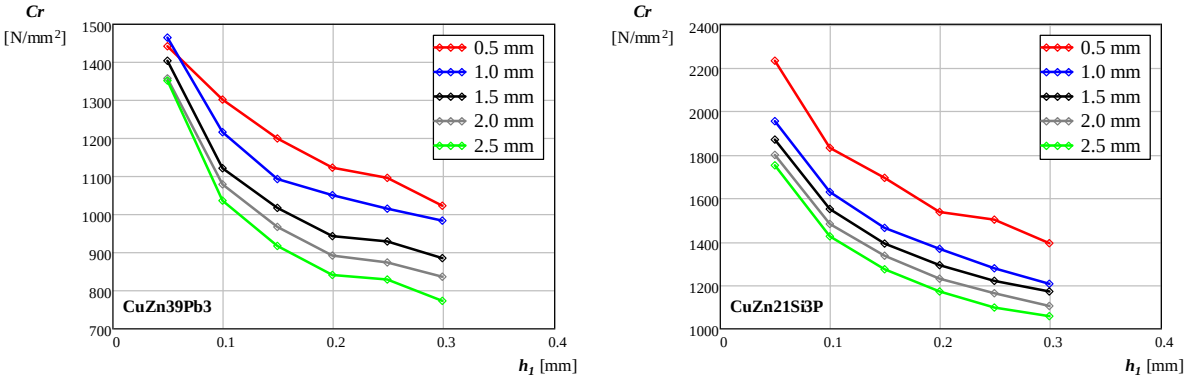


Fig. 10. Cutting resistance $Cr$ as a function of $h_1$ for varying workpiece materials at different depths of cut $a_p$.

As can be seen in Fig. 10 both workpiece materials exhibit a comparatively low cutting resistance if for instance comparing to common steels. It is also evident that CuZn21Si3P exhibits a higher value of the cutting resistance for all machining cases investigated. This difference could be expected to result in more rapid tool deterioration while machining CuZn21Si3P as compared to the more commonly used CuZn39Pb3 lead-alloyed material. As a result, the next step of the investigation was thus to experimentally compare the attained tool wear for each of the two investigated workpiece materials under equivalent machining conditions.

*3.4. Tool wear analysis*

The tool wear analysis were performed through comparing the attained tool wear while longitudinally turning each of the two investigated workpiece materials at $v_c$ = 400 m/min, $f$ = 0.20 mm/rev and $a_p$ = 0.8 mm using uncoated cemented carbide cutting tools. The tool wear attained for CuZn39Pb3 during these experiments can be

found in Fig. 11. The blue curves in the figure illustrate the geometry at a cross section of the tool, the location of which is indicated by the red line in the respective images.

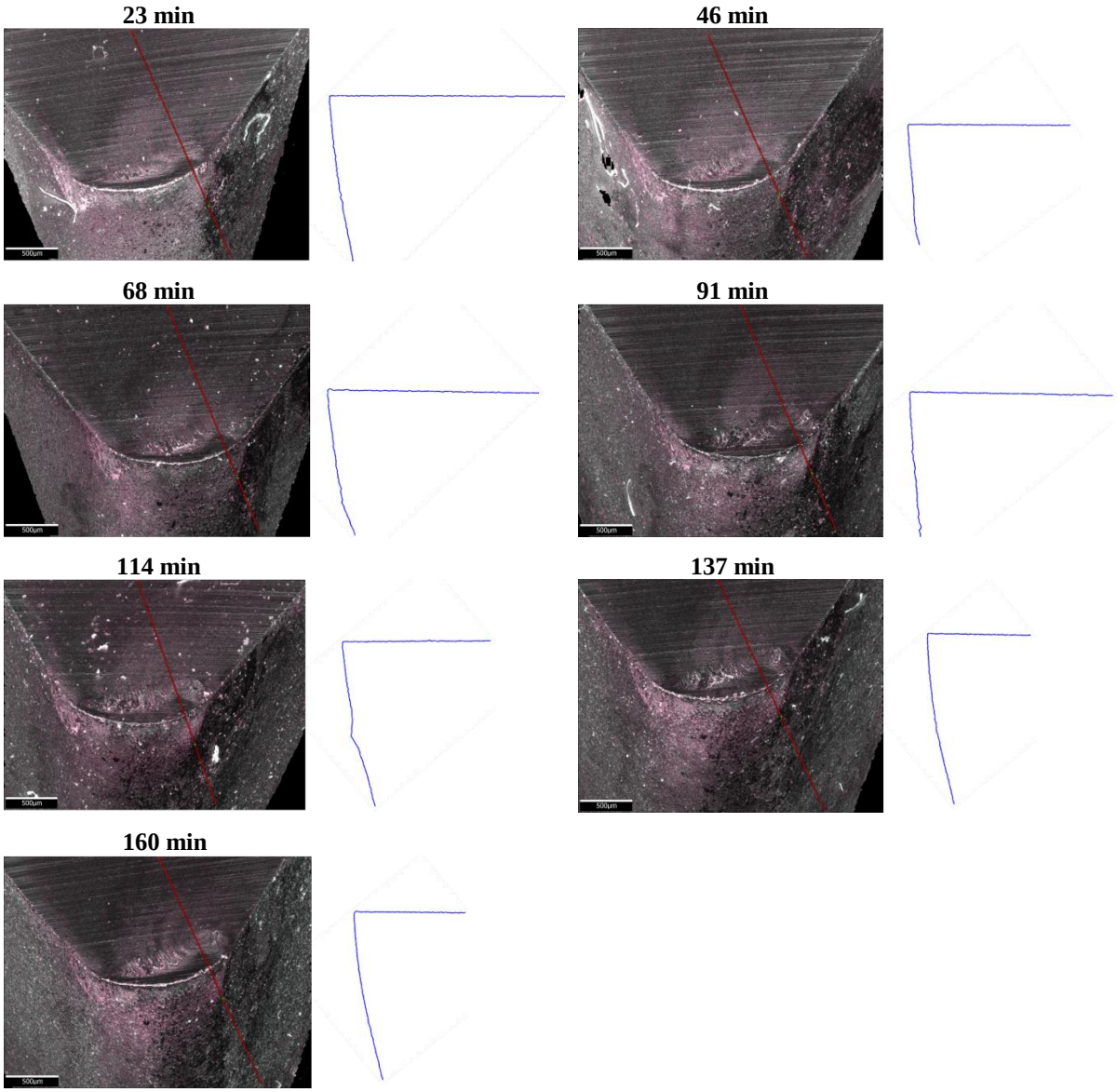


Fig. 11. Attained tool wear as a function of machining time while machining CuZn39Pb3.

As can be seen in Fig. 12 the attained tool wear is minimal, on the verge of nonexistent while machining CuZn39Pb3 even after 160 min of machining. It thus seems plausible to assume that the tool could be used for a substantially longer time while machining CuZn39Pb3 at these process conditions. The corresponding results attained for CuZn21Si3P while using equivalent process conditions can be found in Fig. 12. As can be seen in Fig. 12, machining of CuZn21Si3P under these conditions results in the formation of a crater on the rake face of the cutting tool which grows steadily until the tool fails after approximately 140 min of machining.

As illustrated by the attained results the tool wear while machining the lead-free material CuZn21Si3P is substantially larger at the given process conditions as compared to the case of machining the lead-alloyed CuZn39Pb3 material.

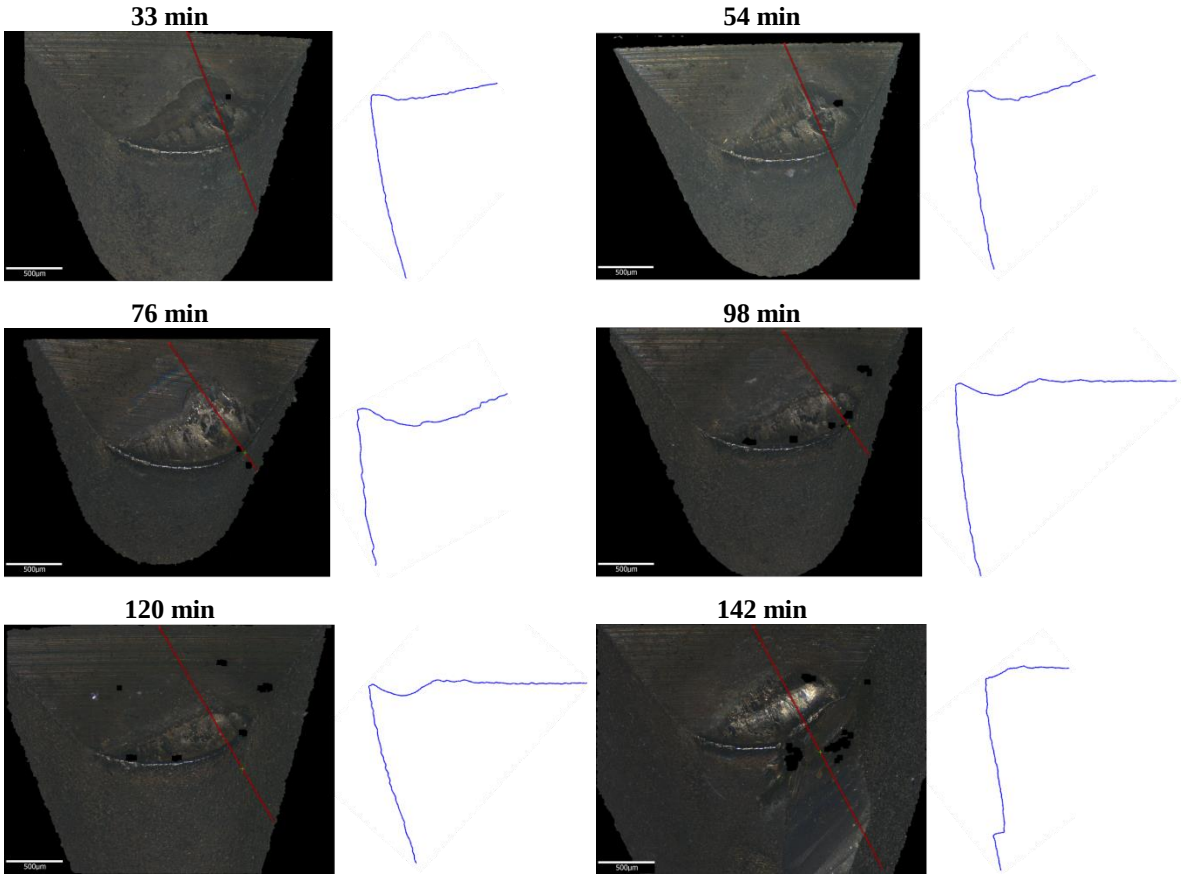


Fig. 12. Attained tool wear as a function of machining time while machining CuZn21Si3P.

## 4. CONCLUSIONS

During the current research it was found that lead-free brass CuZn21Si3P has both a greater strength (yield and tensile) as well as a significantly higher hardness as compared to the lead-alloyed alternative CuZn39Pb3. It was also noted that CuZn21Si3P has a significantly lower thermal conductivity as compared to the lead-alloyed CuZn39Pb3. All of these material properties were based on previous research believed as resulting in a lower machinability for the lead-free material, something which to a certain extent was corroborated by the experimental results attained while machining the two materials. During the current research it was found that while using uncoated cemented carbide tools the attained cutting forces were significantly higher for the lead-free brass as compared to the lead-alloyed alternative during equivalent machining conditions. This difference in cutting forces resulted in a difference of the cutting resistance between the two materials in the range of roughly 200 N/mm$^2$ to 790 N/mm$^2$ depending on machining conditions. This difference in mechanical load could to a certain extent be the reason for the substantial difference in tool wear attained while machining the two materials under equivalent conditions.

## ACKNOWLEDGEMENT

The research presented in this paper is a part of the Lead-Free Brass research project funded by MISTRA, The Swedish Foundation for Strategic Environmental Research, as well as the Swedish Strategic Innovation Area SIO: Produktion2030. It is also a part of the Sustainable Production Initiative cooperation between Lund University and Chalmers University of Technology. The authors would also like to acknowledge the contributions attained from AB Markaryds Metallarmatur.

## REFERENCES

Andersson, M. and J.-E. Ståhl (2007). Polar Machinability Diagram - a Model to Predict the Machinability of a Work Material, *Swedish Production Symposium 2007*, Gothenburg, Sweden

Avdovic, P., L. Xu, M. Andersson and J.-E. Ståhl (2011). Evaluating the Machinability of Inconel 718 using Polar Diagrams, *Journal of Engineering for Gas Turbines and Power*, **133**.

Brennert, S. (1993). *Materiallära*, Karlebo, Liber utbildning AB.

García, P., S. Riviera, M. Palacios and J. Belzunce (2010). Comparative study of the parameters influencing the machinability of leaded brasses, *Engineering Failure Analysis*, **17**, 771-776.

La Fontaine, A. and V.J. Keast (2006). Compositional distributions in classical and lead-free brasses, *Materials Characterization*, **57**, 424-429.

Li, S.F., K. Kondoh, H. Imai and H. Atsumi (2011). Fabrication and properties of lead-free machinable brass with Ti additive by powder metallurgy, *Powder Technology*, **205**. 242-249

Olovsjö, S., P. Hammersberg and L. Nyborg (2011). A method for evaluation of potential machinability correlated with material properties between different batches of material, *The 4th International Swedish Production Symposium*, Lund, Sweden, 250-256.

Olovsjö, S., P. Hammersberg, P. Avdovic, J.-E. Ståhl and L. Nyborg (2012). Methodology for evaluating effects of material characteristics on machinability - theory and statistics-based modelling applied on Alloy 718, *International Journal of Advanced Manufacturing Technology*, **59**, 55-66.

Ren, X. J., R.D. James, E. J. Brookes and L. Wang (2001). Machining of high chromium hardfacing materials, *Journal of Materials Processing Technology*, **115**, 423–429.

Ståhl, J.-E. (2012). *Metal Cutting - Theories and models*. Division of Production and Materials Engineering, Lund University in cooperation with Seco Tools AB, Lund/Fagersta, Sweden.

Taha, M.A., N.A. E-Mahallawy, T.M. Mousa, R.M. Hamouda and A.F.A.G. Yousef (2012). Microstructure and castability of lead-free silicon brass alloys, *Materialwissenschaft und Werkstofftechnik*, **43**, 699-704.

Trent, E. and P. Wright (2000). *Metal Cutting*, Fourth edition, Butterworth-Heinemann, Stoneham, MA, USA.

UNEP, Chemicals Branch, DTIE (2010). *Final review of scientific information on lead*. United Nations Environment Programme.

Wieland-SW1 *Lead-free special brass*. Wieland-Werke AG, www.wieland.de, 2014-01-28.

Wieland-Z32/Z33 *Machining brass*. Wieland-Werke AG, www.wieland.de, 2014-01-28.

Xu, L., Z. Jiang and J.-E. Ståhl (2010). Machinability Prediction of Workpiece Material with a Diagraph Method, *Advanced Material Research*, **97-101**, 2072-2075.

Xu, L., F. Schultheiss, M. Andersson and J.-E. Ståhl (2013). General conception of polar diagrams for the evaluation of the potential machinability of workpiece materials, *International Journal of Machining and Machinability of Materials*, **14**, 24-44.